

EFFECT OF FIBER/MATRIX INTERFACIAL PROPERTIES ON MECHANICAL PROPERTIES OF UNIDIRECTIONAL CRYSTALLINE SILICON CARBIDE COMPOSITES - T. Hinoki, L.L. Snead and E. Lara-Curzio (Oak Ridge National Laboratory), J. Park, Y. Katoh and A. Kohyama (Kyoto University)

OBJECTIVE

The objective of this work is to understand the role of fiber/matrix interfacial strength, including bonding strength and frictional strength, on the properties and behavior of unidirectional silicon carbide matrix composites reinforced with highly crystalline fiber and SiC-based interphase.

SUMMARY

The interfacial properties of CVI-SiC matrix composites reinforced with various fibers (Hi-Nicalon™ Type-S and Tyranno™ SA) and with various fiber/matrix interphase (C, multilayer C/SiC, 'porous' SiC) were evaluated by single fiber push-out testing, compression of double-notched specimens (DNS) and transthickness tensile testing. In turn, these results were correlated with the in-plane tensile stress-strain behavior of the material. The microstructure and fracture surfaces were studied by TEM and SEM. The composites reinforced with Tyranno SA fibers showed brittle fracture behavior, due to large interfacial shear strength and low fiber volume fraction. In the composites reinforced with same fibers, the composites with multilayer C/SiC interphase showed brittle fracture behavior compared with the other composites due to large interfacial shear strength. The transthickness tensile strength of composites reinforced with Hi-Nicalon Type-S fibers was larger than that of composites reinforced with Tyranno SA fibers, although the interlaminar shear strength of both materials determined by DNS was similar.

PROGRESS AND STATUS

Introduction

Silicon carbide has excellent high temperature mechanical properties, chemical stability and low activation properties and therefore SiC/SiC composites are expected to be used as structural material for high temperature industrial and nuclear applications [1,2]. It has been reported that conventional SiC/SiC composites degrade significantly following neutron irradiation due to fiber/matrix interfacial degradation. This degradation has been attributed to shrinkage of the SiC fibers [3] and degradation of the carbon interphase [4]. Therefore, for these materials to be used in nuclear-related applications it will be necessary to develop and evaluate SiC/SiC composites with highly-crystalline SiC fiber and SiC-based fiber/matrix interphases that are expected to be stable to neutron irradiation.

The importance of the fiber/matrix interfacial strength on mechanical properties of CMCs has long been emphasized [5]. The major roles of the interface are the transfer of load between fiber and matrix, and to arrest and deflect crack propagation in the matrix. A balance must be reached, though, to maximize load transfer from the matrix to the fibers and vice versa, while retaining the ability of the fibers to debond and slide. This balance is determined by the magnitude of the interfacial strength at the fiber/matrix interphase. Therefore, to optimize the magnitude of the interfacial strength, the conditions at the interface must be tailored by selecting an appropriate combination of constituents, and perhaps even by modifying the fiber surface topography.

Single fiber push-out test was carried out to evaluate interfacial shear strength including interfacial bonding strength and frictional strength directly. In addition the interlaminar shear strength of these materials was determined by compression of the double-notched specimen (DNS) [7,8]. This simple method was preferred in this work for post-irradiation experiments, since the specimens used in this work would be irradiated by neutrons. Because the state of stress at the fiber/matrix interphase is multiaxial, i.e.- in addition to shear stresses in involves normal tensile stresses, it became necessary to determine the transthickness tensile strength of the material. These properties are controlled by the weakest link among the fiber/matrix interfacial region and the matrix [9].

The objective of this work is to understand the characteristics of the fiber/matrix interfacial strength including bonding strength and frictional strength in unidirectional silicon carbide composites with highly-crystalline fibers and SiC-based interphase. These experimental techniques will be applied to neutron-irradiated experiments. The effects of neutron irradiation on mechanical properties for the composites used in this work will be evaluated in the near future.

Experimental

The materials used in this study were unidirectional SiC fiber-reinforced SiC matrix composites fabricated by isothermal chemical vapor infiltration (ICVI) by Hyper-Therm High-Temperature Composites, Inc. for the ORNL/Kyoto University round robin irradiation program. Fibers used were low-oxygen stoichiometric SiC fibers, Hi-Nicalon™ Type-S [10] and Tyranno™ SA [11,12]. The Tyranno SA fiber used in this work has been identified as “grade 1”. It is a research grade fiber, and its properties are slightly different from Tyranno SA “grade 3” fiber, which currently is commercially available. The tensile strength of grade 1 fibers is 2.0 GPa, while that of grade 3 fibers is larger than 2.5 GPa. Prior to matrix infiltration the fibers were coated with either carbon, multilayer C/SiC or ‘porous’ SiC by CVI. Mixtures of methyltrichlorosilane, argon, methane and hydrogen gases were used to deposit the ‘porous’ SiC interphase onto the fibers. In the multilayer C/SiC interphase, the

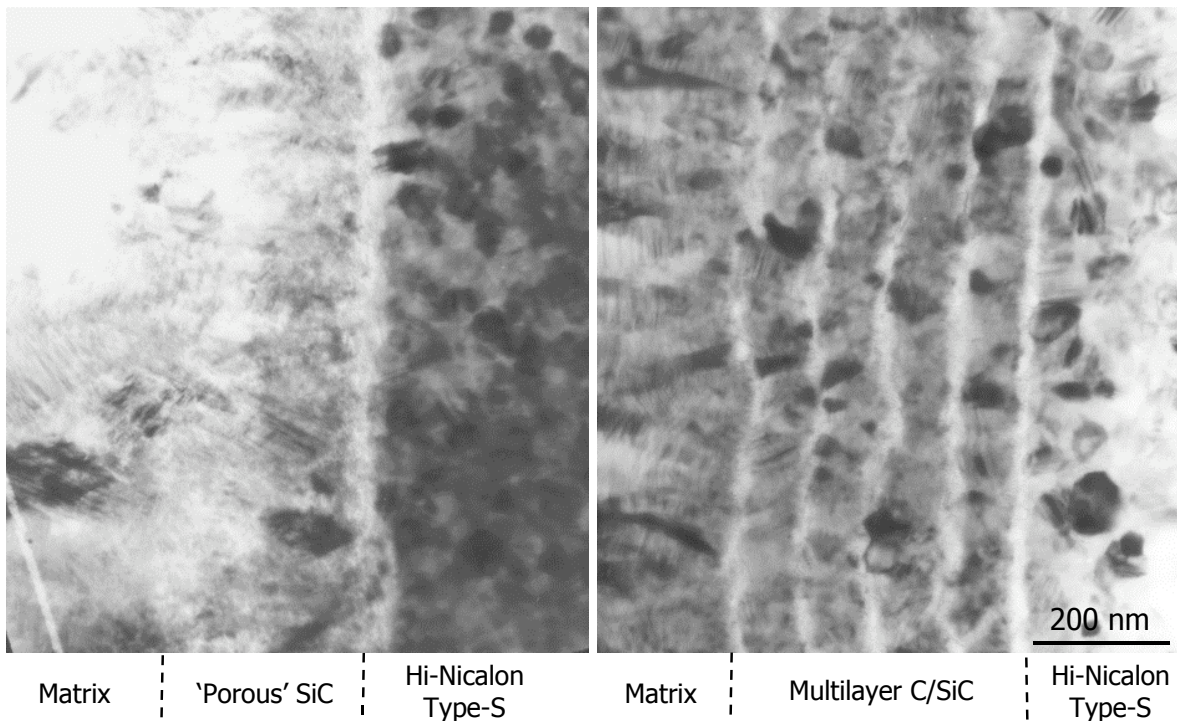


Fig. 1: TEM Images of SiC-based Interphase

first SiC layer was deposited following the deposition of a thin, interrupted layer of pyrolytic C. Four SiC layers were deposited with interrupted pyrolytic C [13]. Transmission electron microscopy (TEM) images of both 'porous' SiC and multilayer C/SiC interphase are shown in Fig. 1. The properties and characteristics of the SiC/SiC composites used in this work are presented in Table I. The thickness of the interphase and fiber volume fraction were estimated from cross sectional SEM images. One of the reasons for the low fiber volume fraction obtained was the extra SiC seal coating applied to the composites, which was 50 μm thick on average.

Table 1: Properties of unidirectional composites

ID	TST1	TST2	TSM	TSP	SAC	SAM
Fiber	Hi-Nicalon™ Type-S				Tyranno™ SA	
F/M interphase	C		Multilayer C/SiC	Porous' SiC	C	Multilayer C/SiC
Interphase Thickness (nm)	520	720	580	380	560	880
Density (Mg/m^3)	2.58	2.58	2.65	2.56	2.55	2.53
V_f (%)	29	29	38	26	21	24
Porosity (%)	19	19	16	19	19	20

Tensile tests were carried out on test specimens with fibers aligned in the loading direction. The test specimens were straight-sided with dimensions 50 mm (long) _ 4 mm (wide) _ 1.5 mm (thick) and the gauge section was 18 mm-long in the middle of the specimen. All tests were conducted at a constant cross-head speed of 10 $\mu\text{m}/\text{sec}$ at ambient temperature. Details of the tensile test are reported elsewhere [14].

The double-notched specimens (DNS) for interlaminar shear strength tests were machined to dimensions 25 mm (long) _ 4.0 mm (wide) _ 1.5 mm (thick) and contained two centrally-located notches, 6 mm apart, that were machined halfway through the thickness using a dicing saw, which is an automatic fine slicer with a diamond-impregnated wheel. The shear tests by compression of DNSs were carried out at ambient temperature at a constant cross-head displacement rate of 10 $\mu\text{m}/\text{sec}$. The specimens were end-loaded using a fixture to provide lateral support to prevent specimen buckling. Fracture surfaces following the tensile tests and the shear tests of DNSs were studied by scanning electron microscopy (SEM).

Interfacial shear properties were obtained by single-fiber push-out tests. Samples were sliced from composite specimens normal to the fiber direction into 500 μm -thick sections, which were mechanically polished to a final thickness of approximately 50 μm . In a thicker specimen, the debond crack typically initiates near the top surface when the fiber is pushed in. Eventually when the debond crack propagates in a stable manner through the entire thickness of the specimen the fiber is pushed out. However when a specimen is sufficiently thin (the thickness depends on interfacial shear strength), the push-in load corresponds to push-out load, i.e.- the debond crack propagates through the thickness of the specimen in an unstable manner. The effect of specimen thickness on single fiber push-out test has been reported elsewhere [6]. For the tests the specimens were mounted on top of a holder containing a groove of 50 μm wide. Isolated fibers with the fiber direction perpendicular to the holder surface on the groove were selected with a video microscope

and were pushed out using a Berkovich-type pyramidal diamond indenter tip with maximum load capability of 1 N.

Transthickness tensile tests were also carried out. The samples were machined to dimensions, 5.0 mm (long) _ 5.0 mm (wide) _ 1.5 mm (thick). The test specimens were adhesively-bonded with epoxy to a pair of holders, with 5 mm square faces. The holders were connected to the load train using a pair of universal joints to promote self-alignment of the load train during the movement of crosshead to minimize sample bending. All tests were conducted with the cross-head speed of 10 $\mu\text{m}/\text{sec}$ at ambient temperature.

Results

The results of tensile testing revealed that both the average ultimate tensile strength (UTS) and proportional limit stress (PLS) of Hi-Nicalon Type-S specimens were larger than those of Tyranno SA specimens. PLS was obtained from using the 0.01 % strain offset criterion. The average modulus of elasticity, obtained from the linear region of the stress-strain curve, of composites reinforced with Tyranno SA fibers was larger than that of composites reinforced with Hi-Nicalon Type-S fibers. Composites reinforced with Hi-Nicalon Type-S showed short fiber pull-out, while composites reinforced with Tyranno SA fibers showed brittle fracture behavior as shown in Fig. 2. It was also found that the tensile properties and fracture behavior of these composites were affected by the fiber/matrix interphase. The magnitude of the UTS, the PLS and modulus of elasticity for composites containing multilayer C/SiC interphase was smaller than that of the other composites. Composites with multilayer C/SiC interphase were brittle compared to composites with the other interphase. The tensile results are presented in Table 2.

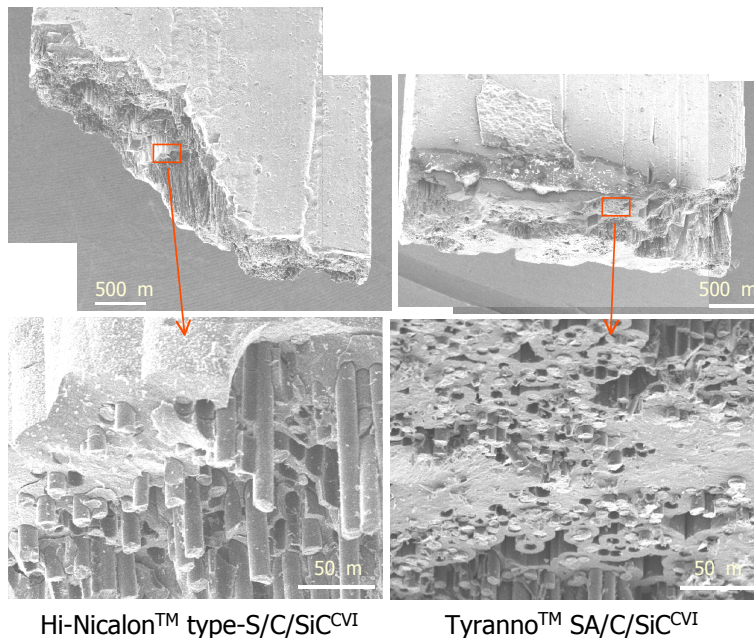


Fig. 3 shows a typical cross head displacement vs. shear stress curve obtained from the compression of a DNS specimen and a crack path in a DNS following a test. The resulting cross

head displacement vs. shear stress curves obtained from the compression of a DNS specimen

Table 2: Summary of mechanical properties

ID	TST1	TST2	TSM	TSP	SAC	SAM
Tensile modulus (GPa)	336	306	256	307	417	350
Flexural modulus (GPa)	296	284	237	260	219	205
Tensile PLS (MPa)	339	268	229	276	220	148
Flexural PLS (MPa)	490	533	356	422	214	199
UTS (MPa)	442	319	229	282	220	148
Flexural strength (MPa)	907	748	757	485	255	199
Shear strength (MPa)	62.8	64.1	60.7	85.8	65.8	56.7
Interfacial shear stress (MPa)	163	149	180	212	211	341
Transthickness tensile strength (MPa)	26.9	-	-	-	20.2	-

were slightly parabolic up to the peak load which was followed by a sudden load drop when the specimens failed. The apparent shear strength (τ) was determined from Eq. 1, as the ratio of the peak load, P_{max} , divided by the surface area of the imaginary plane between the notches.

$$\tau = \frac{P_{max}}{wL} \quad (1)$$

where w is the specimen width and L is the notch separation. It was found that there were no significant differences among the shear strength values obtained for the composites evaluated except for the composites reinforced with Hi-Nicalon Type-S fibers and with 'porous' SiC interphase (Fig. 4). The shear strength of composites with multilayer C/SiC interphases was slightly smaller than that of composites with the other interphases.

The interfacial shear strength (ISS) (τ_{is}) of these materials was approximated from the 'push-out' load (P) in single fiber push-out testing and calculated from Eq. 2.

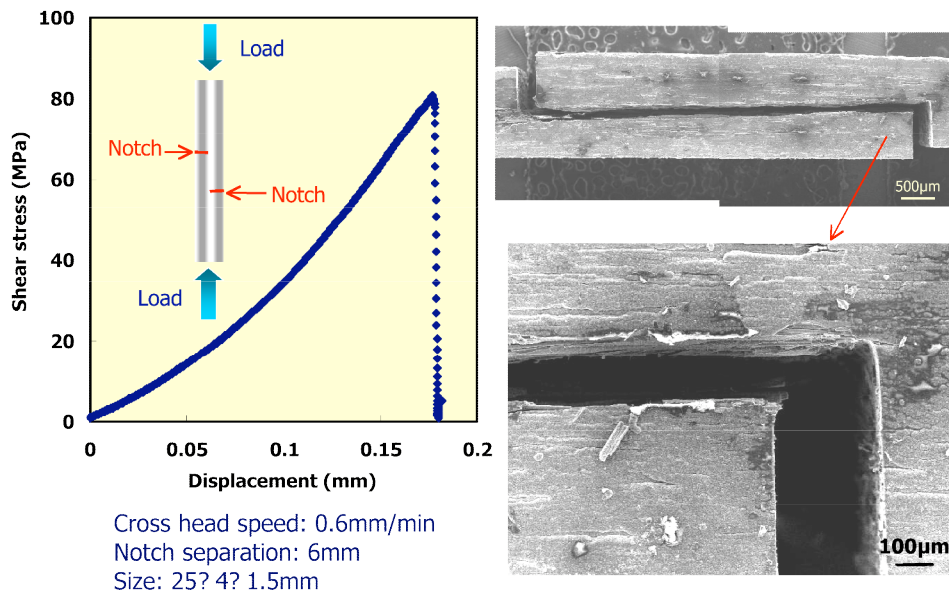


Fig. 3: A Loading Curve and a Crack Path of DNS Shear Test

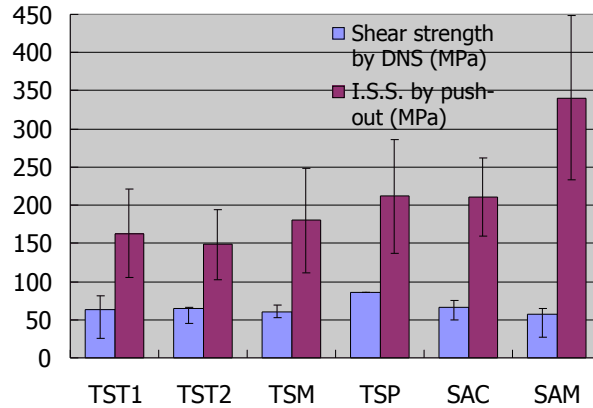


Fig. 4: Effect of fiber and interphase properties on shear strength and interfacial shear strength

$$\tau_{is} = \frac{P}{\pi D t} \quad (2)$$

where τ_{is} is D is fiber diameter and t is specimen thickness. Although this is only an approximation, the objective of these tests was establishing a simple procedure for evaluating the effect of neutron irradiation on the interfacial properties of SiC/SiC composites. The results from ISS are compared with those from shear strength testing of DNS in Fig. 4. Error bars of the ISS represent one standard deviation about the mean value whereas the error bars in the DNS shear strength data represent maximum and minimum values. Although the state of stress in these two test configurations are very different, and therefore a direct comparison may not be appropriate, the results obtained from these tests will provide the means for identifying changes in the interfacial properties of these materials that may be induced by neutron irradiation. For composites with the same interphase, the ISS of composites reinforced with Tyranno SA fibers was slightly larger than that of composites reinforced with Hi-Nicalon Type-S fibers. In composites reinforced with same fiber, the ISS of composites with multilayer C/SiC interphase and 'porous' SiC interphase was slightly larger than that of composites with C interphase.

A typical fracture surface and crack path for a transthickness tensile test specimen are shown in Fig. 5. It was found that in this test the crack propagated interlaminarly between large pores in the

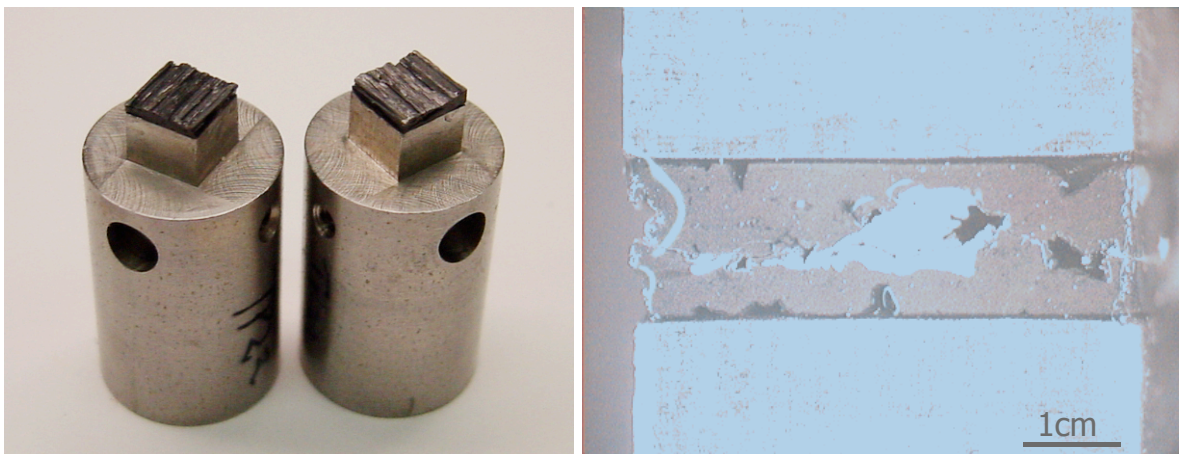


Fig. 5: Fracture surface and crack path of transthickness tensile specimen

matrix. The cross head displacement vs. stress curves obtained from transthickness tensile testing were slightly parabolic up to the peak load which was followed by a sudden load drop when the specimens failed as shown in Fig. 6. Average transthickness tensile strength of SAC (Tyranno SA/C/SiC) and TST1 (Hi-Nicalon Type-S/C/SiC) composites was 20.2 MPa and 26.9 MPa, respectively. Mechanical properties are summarized in Table 2.

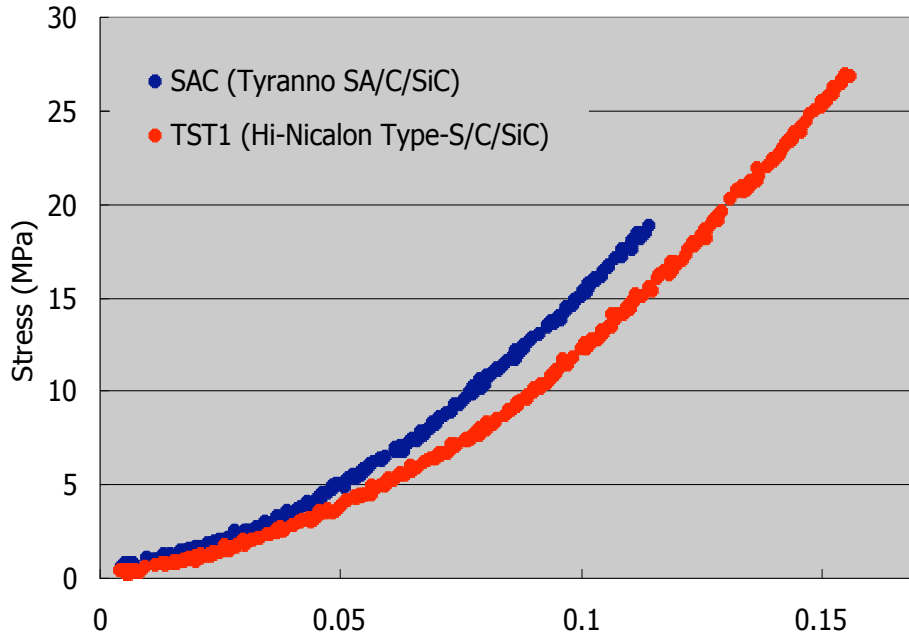


Fig. 6: Effect of fiber on displacement vs. stress curves of transthickness tensile tests

Discussions

The ISS of composites reinforced with Tyranno SA fibers obtained from single fiber push-out tests was larger than that of composites reinforced with Hi-Nicalon Type-S fibers and similar interphase. These differences can be explained from the differences in the surface topography of these fibers as a result of the differences in grain sizes. The surface roughness of these fibers was evaluated quantitatively by Micromap system. Fig. 7 shows the surface height of the single fibers, respectively. 'Rq' in the figure means the Root-Mean-Square (RMS) surface height. The average RMS surface height of Hi-Nicalon Type-S and Tyranno SA was 0.87 and 1.72 nm, respectively. These results are consistent with the difference in tensile behavior that was observed between composites reinforced with these two fibers, particularly the differences in the magnitude of fiber pull-out observed during fractographic examination which is related to the magnitude of the interfacial shear stress according to:

$$h = \frac{\sigma_m^2 r}{2\tau} \quad (3)$$

where h is pullout length, σ_m is matrix cracking stress, r is fiber radius and τ is interfacial shear strength. The matrix cracking stress and the fiber diameter of composites reinforced with Tyranno SA fibers are smaller and the interfacial shear strength of the composites is larger than that of the composites reinforced with Hi-Nicalon Type-S fibers. So pull-out length of composites reinforced

with Tyranno SA fibers should be shorter than that of the composites reinforced with Hi-Nicalon Type-S fibers.

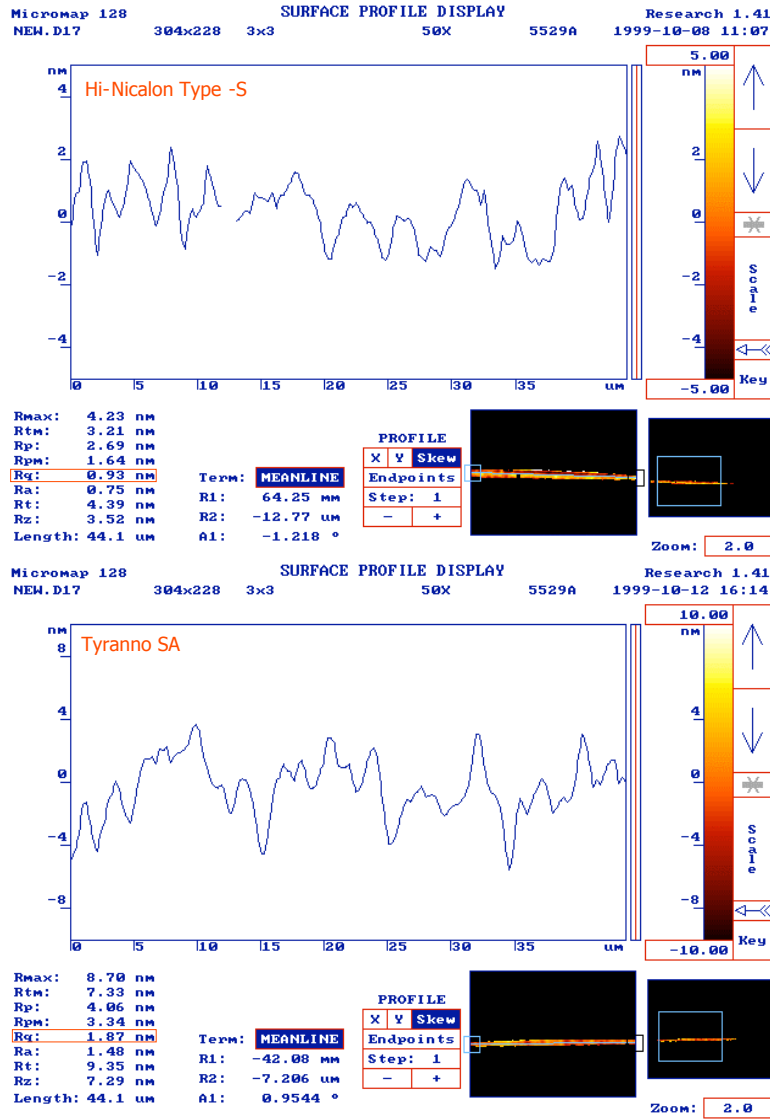


Fig. 7: Surface roughness of the fibers, Hi-Nicalon Type-S and Tyranno SA (grade 1)

The theoretical modulus of composites (E_c) is calculated from Eq. 4.

$$E_c = V_f E_f + V_m E_m \quad (4)$$

where E_f and E_m are moduli of fiber and matrix, V_f and V_m are volume fractions of fiber and matrix. From this calculation, the moduli of the composites used in this study must be comparable and in the case of composites reinforced with Hi-Nicalon Type-S and Tyranno SA fibers containing C interphase should be 363 GPa. However the modulus of the composites reinforced with Tyranno SA fibers is larger than that of the composites reinforced with Hi-Nicalon Type-S. The modulus of composites reinforced with Tyranno SA fibers is larger than the modulus obtained from Eq. 4 and

therefore, it is likely that the actual modulus of Tyranno SA fiber is larger than the value reported by the manufacturer.

In composites reinforced with the same fiber, the magnitude of the ISS for composites containing multilayer C/SiC interphase and 'porous' SiC interphase was larger than that of composites containing C interphase. In the particular case of composites reinforced with Tyranno SA and multilayer C/SiC interphases, the magnitude of the ISS was much larger than of composites containing C interphases. In composites with multilayer C/SiC interphase, the fiber surface roughness is reflected in the rough features of the fracture surface with large interfacial frictional strength, since the first C layer is very thin. The results of ISS do not correlate with the results of DNS shear strength. Shear strength by DNS is affected by porosity, fiber volume fraction and pore size. To understand the different trends between ISS and DNS shear strength, further investigations are required.

There was no significant effect of fiber type on the magnitude of the interlaminar shear strength determined by the compression of double-notched specimens. However, the transthickness tensile strength of composites reinforced with Hi-Nicalon Type-S fibers was much larger than that of composites reinforced with Tyranno SA fibers. DNS shear strength is affected by the roughness of fracture surface, while transthickness tensile strength does not affected significantly. Porosity of composites reinforced with Hi-Nicalon Type-S fibers was lower than that of composites reinforced with Tyranno SA fibers. The average pore size of composites reinforced with Tyranno SA fibers seemed larger than that of composites reinforced with Hi-Nicalon Type-S fibers. These results induce that the large interfacial strength of composites reinforced with Tyranno SA fibers is attributed to larger interfacial frictional strength.

CONCLUSIONS

- (1) The interfacial frictional stresses were larger in composites reinforced with Tyranno SA fibers than in composites reinforced with Hi-Nicalon Type-S fibers, and this difference was explained based on the difference in surface topography between these fibers. As a result, composites reinforced with Tyranno SA fibers showed brittle fracture behavior compared with composites reinforced with Hi-Nicalon Type-S fibers. It was also found that the interfacial bonding in composites reinforced with Hi-Nicalon Type-S was larger than that of composites reinforced with Tyranno SA fibers.
- (2) Composite materials containing multilayer C/SiC interphases exhibited less and shorter fiber pull-out and brittler behavior than composites containing other interphases, since the average interfacial shear strength in composites with multilayer C/SiC interphases is larger than that of composites containing C interphases. It was found that the magnitude of the difference of interfacial shear strength was the largest for composites reinforced with Tyranno SA fibers.

ACKNOWLEDGEMENT

This work was supported by Japan-USA Program of Irradiation Test for Fusion Research (JUPITER) and by Core Research for Evolutional Science and Technology (CREST) program under the title of "R & D of Environment Conscious Multi-Functional Structural Materials for Advanced Energy Systems".

REFERENCES

- [1] P. Fenici, A.J. Frias Rebelo, R.H. Jones, A. Kohyama and L.L. Snead, *J. Nucl. Mater.*, 258-263 (1998) 215.
- [2] L.L. Snead, R.H. Jones, A. Kohyama and P. Fenici, *J. Nucl. Mater.*, 233-237 (1996) 26-36.
- [3] G.W. Hollenberg, C.H. Henager, Jr., G.E. Youngblood, D.J. Trimble, S.A. Simonson, G.A. Newsome and E. Lewis, *J. Nucl. Mater.*, 219 (1995) 70-86.
- [4] J.H.W. Simmons, *Radiation Damage in Graphite*, Pergamon Press, (1965).
- [5] E. Lara-Curzio and M. K. Ferber, *Numerical Analysis and Modeling of Composite Materials*, Ed. J. W. Bull, Blackie Academic & Professional (1995) 357-399.
- [6] T. Hinoki, W. Zhang, A. Kohyama, S. Sato and T. Noda, *J. Nucl. Mater.*, 258-263 (1998) 1567-1571.
- [7] E. Lara-Curzio and M.K. Ferber, *Thermal and Mechanical Test Methods and Behavior of Continuous-Fiber Ceramic Composites*, ASTM STP 1309, Edited by M.G. Jenkins, S.T. Gonczy, E. Lara-Curzio, N.E. Ashbaugh and L.P. Zawada, American Society for Testing and Materials, (1997) 31-48.
- [8] E. Lara-Curzio and M. Singh, *J. Mater. Sci. Lett.*, 19 (2000) 657-661.
- [9] E. Lara-Curzio, *Comprehensive Composites Encyclopedia*, Elsevier, (2000) 533-577.
- [10] M. Takeda, A. Urano, J. Sakamoto and Y. Imai, *J. Nucl. Mater.*, 258-263 (1998) 1594-1599.
- [11] T. Ishikawa, Y. Kohtoku, K. Kumagawa, T. Yamamura and T. Nagasawa, *Nature*, 391 (1998) 773-775.
- [12] T. Ishikawa, S. Kajii, T. Hisayuki, K. Matsunaga, T. Hogami and Y. Kohtoku, *Key Eng. Mater.*, 164-165 (1999) 15-18.
- [13] L.L. Snead, M.C. Osborne, R.A. Lowden, J. Strizak, R.J. Shinavski, K.L. More, W.S. Eatherly, J. Bailey and A.M. Williams, *J. Nucl. Mater.*, 253 (1998) 23-30.
- [14] T. Hinoki, L.L. Snead, E. Lara-Curzio, Y. Katoh and A. Kohyama, *Fusion Materials Semi-Annual Progress Reports*, DOE/ER-0313/29 (2000) 74-84.